

## Quantum confinement in porous silicon

Xin Jian Li\*

Structure Research Laboratory, University of Science and Technology of China, Hefei 230026, People's Republic of China  
and Department of Physics, Zhengzhou University, Zhengzhou 450052, People's Republic of China

Yu Heng Zhang

Structure Research Laboratory, University of Science and Technology of China, Hefei 230026, People's Republic of China  
(Received 23 August 1999)

Two emission bands were simultaneously observed in iron-passivated porous silicon and their peak energies were in good agreement with the first two gap energies calculated for silicon nanocrystallites (*nc*-Si). This result indicates the existence of separate conduction subbands caused by the quantum confinement of carriers in *nc*-Si. It was also found that under the frame of the quantum confinement effect, the distribution of the photoluminescence intensity over emission wavelength could be well explained by the size distribution of *nc*-Si. These facts support the quantum confinement model of the luminescence in porous silicon.

The discovery of light-emitting porous silicon<sup>1</sup> (PS) and the encouraging progress in fabricating PS-based light emitters<sup>2-5</sup> have cast a new light on Si-based optoelectronics. However, the progress on raising the photoluminescence (PL) intensity<sup>6</sup> and on preventing the PL degradation and the up-shift of the PL peak energy<sup>7-9</sup> is very slow. On the other hand, the origin of the PL in PS is still controversial.<sup>10</sup> Presently, although the quantum confinement model<sup>1</sup> (QCM) seems most acceptable,<sup>10-15</sup> supports for other models could still be found in some very recently published papers.<sup>16-18</sup> As early as in 1992, F. Buda *et al.* had calculated the electronic structure of silicon nanocrystallites (*nc*-Si) and predicted the existence of separate conduction subbands (sub-CB) in such a confined system.<sup>14</sup> According to their theory, a multiband emission should be observed in PS and this might have provided a criterion to distinguish QCM from the other models. But this prediction, the multiband emission, has not been observed till today. In this letter, we report that two emission bands, which might originate from the radiative recombination of carriers from two separate sub-CB of *nc*-Si, were simultaneously observed in iron-passivated PS (IPS). Additionally, it was also found that under the frame of QCM, the distribution of the PL intensity over the emission wavelength excited by the corresponding most efficient wavelengths could be well explained by the size distribution of *nc*-Si. All the above results provide strong evidences for QCM of the PL in PS.

IPS has been previously shown to exhibit nondegrading PL with a stable PL peak energy, its PL peak intensity is typically 2–2.5 times stronger than that of normal PS.<sup>13</sup> The above properties of IPS provided good conditions for investigating its PL mechanism. In this paper, all the samples were prepared according to the method given in Ref. 13.

Figure 1(a) presents the PL spectra of seven different IPS samples. Obviously, all these spectra exhibit two emission bands, a strong one in red range and a weak one in ultraviolet range. The peaks of the red bands range from ~670 to ~760 nm (~1.63–~1.85 eV) while those of the ultraviolet bands range from ~330 to ~360 nm (~3.44–~3.76 eV), depending upon the different preparation conditions. But blue-green

emissions were observed neither in the freshly prepared samples nor in the annealed samples. The coexistence of the two emission bands implies that above the enlarged band gap of *nc*-Si at least two energy levels in the conduction band (CB) were formed in the case of IPS. In other words, instead of the continuous CB of bulk Si, a series of separate sub-CB were formed in *nc*-Si because of the space confinement on carriers. Accordingly, the observed two emission bands correspond to the electron transition from the first sub-CB (with the lowest energy level) and the second sub-CB (with the second lowest energy level) to the valence band (VB), re-

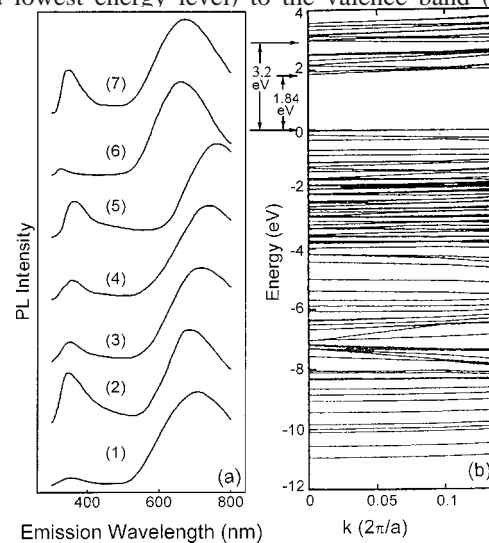


FIG. 1. (a) The PL spectra of IPS samples prepared by the method described in Ref. 13. The resistivity of the initial silicon wafers is ~0.6–0.9  $\Omega$  cm for (1), (2), (3), (4), (5) and ~1.5–2.0  $\Omega$  cm for (6), (7). The adopted  $\lambda_{EX}$  and filter are 210 nm and #310, respectively. The samples are (1) freshly prepared and annealed in ambient air for 0.5 h at 150 °C (2), 200 °C (3), 300 °C (4), 400 °C (5), and exposed to ambient air at room temperature for 2.5 months (6), 4 months (7), respectively. (b) Band structure of a ~1 nm-wide silicon quantum wire along the one-dimensional Brillouin zone near  $k=0$ . The arrows indicate the top of the valence band and the bottoms of the first and the second sub-CB, respectively. This result is taken from Ref. 14.

spectively. These results qualitatively agree with the theoretical calculation of the band structure for *nc*-Si by Buda, Kohanoff, and Parrinello<sup>14</sup> which was carried out on the basis of QCM. As is shown in Fig. 1(b), Their results indicate that for  $k=0$ , the CB of *nc*-Si is composed of several separate sub-CB, with the bottoms of the first and the second sub-CB locating at  $\sim 1.84$  and  $\sim 3.2$  eV, respectively.

Based on the above analysis, the PL process in IPS could be described as the followings. When a photon with certain wavelength  $\lambda_{EX}$  is absorbed by an electron at the top of VB, the electron will be excited to a high-energy state with  $E_{EX} = h/\lambda_{EX}$ . Then the electron will partly transfer its energy to phonons and relax to the first or the second sub-CB. Finally, the electron will transit back to VB and simultaneously emits a photon. Since the energy level of the first sub-CB is lower, the electrons would most probably transit back to VB from this subband and this recombination corresponds to the stronger luminescence in red range. Similarly, the energy level of the second sub-CB is higher, the transition probability of the electron will be much smaller and this recombination corresponds to the weaker luminescence in ultraviolet range. So if the total PL intensity of a sample is not strong enough, the ultraviolet emission will be very weak and might be completely submerged in the noise. That is why the ultraviolet emission band is difficult to be co-observed with the visible emission band in normal PS.

Since it has been proved that both Fe-Si bonds and  $\alpha$ -Fe<sub>2</sub>O<sub>3</sub> presented in IPS,<sup>13</sup> it is important to carry out the PL measurement on them. No similar luminescence bands were observed in the above materials. Therefore, the possibility that the PL might originate from these materials is excluded. What should be mentioned is, single ultraviolet emission band was observed by other groups in annealed PS samples, and it was generally attributed to the covered silicon oxide layer.<sup>19–21</sup> This should not be the case of IPS, because the coverage layer of IPS is not composed of silicon oxide.<sup>13</sup>

Also, an additional support of QCM comes from our experiments of the PL excitation (PLE) spectra, which were obtained by measuring the PL intensity at a fixed emission wavelength ( $\lambda_{EM}$ ) with changing the excitation wavelength ( $\lambda_{EX}$ ) continuously from 210 to 460 nm. Figure 2(a) represents a group of the PLE spectra of a typical IPS sample. Obviously, all these PLE spectra have two peaks, a low-energy peak  $P_1$  and a high-energy peak  $P_2$ , corresponding to the wavelength locations of two most efficient  $\lambda_{EX}$  for the fixed  $\lambda_{EM}$ . Figure 2(b) depicts the variation of the PL intensity of  $P_1$  with emission energy ( $E_{EM}$ ). According to QCM,<sup>1</sup> the PL intensity at certain  $\lambda_{EM}$  ( $E_{gap} = h/\lambda_{EM}$ ) should be decided by the amount of the *nc*-Si with a definite size. So the distribution of the PL intensity given in Fig. 2(b) should represent the size distribution of the *nc*-Si in IPS. This deduction was proved by the experiment of high-resolution transmission electron microscope (HRTEM). Figure 3(a) is a typical HRTEM image of IPS, from which one can see that the size of the *nc*-Si ranged from  $\sim 1$  to  $\sim 6.25$  nm. In Fig. 3(b), we give the size distribution of *nc*-Si, which was obtained by performing statistics over 10 similar regions like Fig. 3(a). The curve given in Fig. 3(b) is the fitting line of the size distribution for the *nc*-Si below 5 nm. As is known, 5 nm is the theoretical up limit for the luminescent

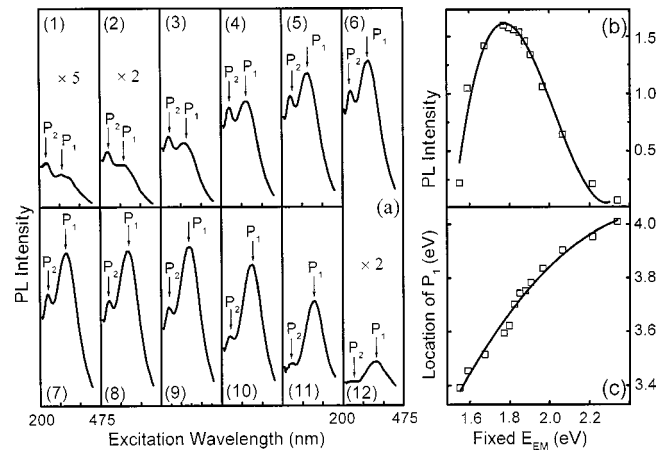


FIG. 2. (a) The evolution of the PLE spectra with the variation of the detected  $\lambda_{EM}$ . The  $\lambda_{EM}$  are chosen as (1) 530 nm, (2) 560 nm, (3) 600 nm, (4) 630 nm, (5) 650 nm, (6) 660 nm, (7) 670 nm, (8) 680 nm, (9) 700 nm, (10) 740 nm, (11) 780 nm, and (12) 800 nm, respectively. The arrows indicate the two excitation peaks. (b) The variation of the PL peak intensity at the detected  $E_{EM}$  (open square) with  $P_1$  and the fitting curve. (c) The blue shift of the most efficient  $E_{EX}$  ( $P_1$ ) with the detected  $E_{EM}$  (open square) and the fitting curve.

*nc*-Si.<sup>14,22–24</sup> It is easy to find that the fitting line of the size distribution [the curve in Fig. 3(b)] and the distribution of the PL intensity versus  $E_{EM}$  [Fig. 2(b)] is similar. This similarity indicates that the PL in IPS is directly resulted from the band-to-band recombination of carriers. Further data analysis to Fig. 2(a) disclose that with the measured  $\lambda_{EM}$  becomes longer,  $P_1$  exhibits an obvious red-shift, as shown in Fig. 2(a). This fact implies that the *nc*-Si with different sizes occupy different most-efficient  $E_{EX}$ ; i.e., the smaller the *nc*-Si size, the higher the most-efficient  $E_{EX}$ . From the above results, the following conclusions could be reached: (1) the emission with bigger  $E_{EM}$  comes from the *nc*-Si with smaller size; (2) the PL intensities at different  $E_{EM}$  is mainly decided by the quantities of the *nc*-Si with corresponding sizes. All these results indicate that the PL in IPS is highly sensitive to the size of *nc*-Si and therefore provide an additional support for QCM.

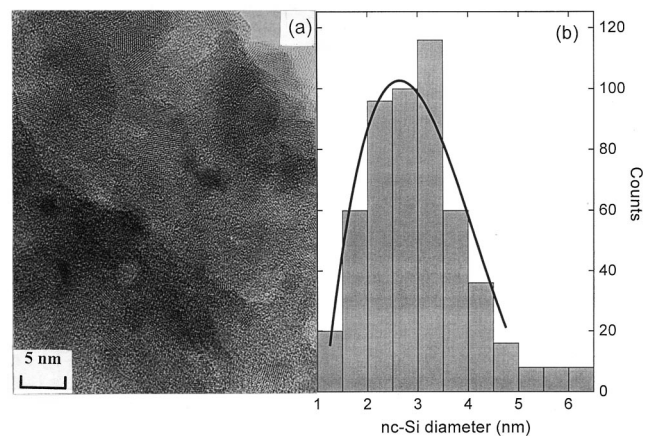


FIG. 3. (a) A typical HRTEM image of IPS. (b) The size distribution of the *nc*-Si (bar) deduced by performing statistics over 10 similar regions as given in (a), with the line as the fitting result for the *nc*-Si below 5 nm.

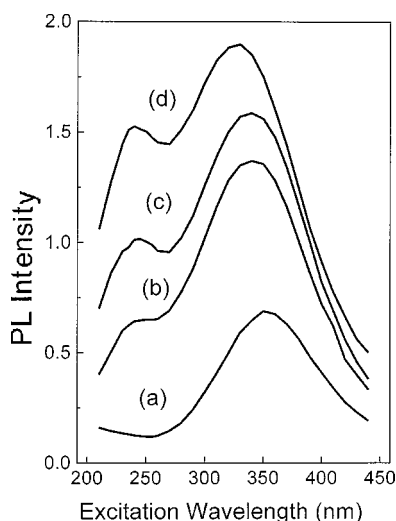


FIG. 4. Time-evolution PLE spectra for a typical IPS sample. (a) Fresh sample and (b), (c), and (d) exposed to ambient air at room temperature for 1, 2, and 4 months, respectively.

The peak position of  $P_2$  in Fig. 2(a) ranges from  $\sim 239.3$  to  $\sim 244.4$  nm ( $\sim 5.07$ – $\sim 5.18$  eV). The largest difference of their peak energies is  $\sim 0.11$  eV, which is much smaller than that of  $P_1$  ( $\sim 0.62$  eV). As far as our knowledge,  $P_2$  is only observed in the PLE spectra of IPS. Figure 4 depicts the time evolution of the PLE spectra for a typical IPS sample when it was exposed to ambient air at room temperature. Clearly,  $P_2$  was not detected in fresh IPS samples, but with time going on,  $P_2$  appeared and gradually increased. This phenomenon occurred synchronously with the increment of the amount of the Fe-Si bonds in IPS during air exposure.<sup>13</sup> Therefore, it is

reasonable to relate the present of  $P_2$  to the present of the Fe-Si layer in IPS. Since the possibility that the PL comes from Fe-Si alloy has been experimentally excluded, the whole PL process under  $P_2$  excitation could be understood as the followings. When an electron in Fe-Si layer absorbs a photon (with  $E_{EX} = 5.07$ – $5.18$  eV), the electron will be excited to a high-energy state related to Fe-Si. Through interacting with phonons, the electron will penetrate the several angstrom-thick Fe-Si layer into the  $nc$ -Si and partly transfer its energy to the phonons in  $nc$ -Si. With the energy further decaying down, the electron will relax to the first or the second sub-CB of the  $nc$ -Si. This above process is a nonradiative recombination process. Finally, the electron will transit back to the VB through emitting a photon. This is a radiative recombination process. Because the main action of the Fe-Si layer is to passivate the surface dangling bonds and therefore the layer thickness for the  $nc$ -Si with different sizes are all of several angstroms, the locations of the best absorption energy  $E_{EX}$  of  $P_2$  for different  $E_{EM}$  are almost of same value.

In conclusion, two emission bands were simultaneously observed in the PL spectra of IPS and were attributed to the formation of separate sub-CB in  $nc$ -Si, one of the most essential effect for a confined system. This result is qualitatively in agreement with the theoretical calculations. The investigations on the PLE spectra and the size distribution of  $nc$ -Si indicate that the PL is highly size-sensitive and the emission process is most probably a band-to-band recombination. Strong experimental evidences of QCM of the PL in IPS were provided in the above viewpoints.

This work was supported by the National Natural Science Foundation of China.

\*Author to whom correspondence should be addressed. Electronic address: lixj@mail.zzu.edu.cn

<sup>1</sup>L. T. Canham, Appl. Phys. Lett. **57**, 1046 (1990).

<sup>2</sup>A. Loni, A. J. Simons, T. I. Cox, P. D. J. Calcott, and L. T. Canham, Electron. Lett. **31**, 1288 (1995).

<sup>3</sup>S. Lazarouk, P. Jaguiro, S. Katsouba, G. Masini, S. La Monica, G. Maiello, and A. Ferrari, Appl. Phys. Lett. **68**, 1646 (1996).

<sup>4</sup>L. Tsybeskov, S. P. Duttgupta, K. D. Hirschman, and P. M. Fauchet, Appl. Phys. Lett. **68**, 2058 (1996).

<sup>5</sup>K. D. Hirschman, L. Tsybeskov, S. P. Duttgupta, and P. M. Fauchet, Nature (London) **384**, 338 (1996).

<sup>6</sup>H. Koyama, T. Nakagama, T. Ozaki, and N. Koshida, Appl. Phys. Lett. **65**, 1656 (1994).

<sup>7</sup>D. W. Cooke, B. L. Bennett, E. H. Farnum, W. L. Hults, K. E. Sickafus, J. F. Smith, J. L. Smith, T. N. Taylor, and P. Tiwari, Appl. Phys. Lett. **68**, 1663 (1996).

<sup>8</sup>L. T. Canham, M. R. Houlton, W. Y. Leong, C. Pickering, and J. M. Keen, J. Appl. Phys. **70**, 422 (1991).

<sup>9</sup>M. A. Tischler, R. T. Collins, J. H. Stathis, and J. C. Tsang, Appl. Phys. Lett. **60**, 639 (1992).

<sup>10</sup>A. G. Cullis, L. T. Canham, and P. D. J. Calcott, J. Appl. Phys. **82**, 909 (1997).

<sup>11</sup>A. G. Cullis and L. T. Canham, Nature (London) **353**, 335 (1991).

<sup>12</sup>T. K. Sham, D. T. Jiang, I. Couthard, J. W. Lorimer, X. H. Feng, K. H. Tan, S. P. Frigo, R. A. Rosenberg, D. C. Houghton, and B. Bryskiewicz, Nature (London) **363**, 331 (1993).

<sup>13</sup>Y. H. Zhang, X. J. Li, L. Zheng, and Q. W. Chen, Phys. Rev. Lett. **81**, 1710 (1998).

<sup>14</sup>F. Buda, J. Kohanoff, and M. Parrinello, Phys. Rev. Lett. **69**, 1272 (1992).

<sup>15</sup>G. Polisski, H. Heckler, D. Kovalev, M. Schwartzkopff, and F. Koch, Appl. Phys. Lett. **73**, 1107 (1998).

<sup>16</sup>M. V. Wolkin, J. Jorne, P. M. Fauchet, C. Delerue, and G. Allan, Phys. Rev. Lett. **82**, 197 (1999).

<sup>17</sup>T. Wadayama, T. Arigane, and A. Hatta, Appl. Phys. Lett. **73**, 2570 (1998).

<sup>18</sup>T. Inokuma, Y. Wakayama, T. Muramoto, R. Aoki, Y. Kurata, and S. Hasegawa, J. Appl. Phys. **83**, 2228 (1998).

<sup>19</sup>D. T. Jiang, I. Coulthard, T. K. Sham, J. W. Lorimer, S. P. Frigo, X. H. Feng, and R. A. Rosenberg, J. Appl. Phys. **74**, 6335 (1993).

<sup>20</sup>J. Zuk, R. Kuduk, M. Kulik, J. Liskiewicz, D. Maczka, P. V. Zhukovski, V. F. Stelmakh, V. I. Bondarenko, and A. M. Dorofeev, J. Lumin. **57**, 57 (1993).

<sup>21</sup>Qianwang Chen, Guien Zhou, Jingsheng Zhu, Chenggao Fan, X.-G. Li, and Y. Zhang, Phys. Lett. A **224**, 133 (1996).

<sup>22</sup>B. Delley and E. F. Steigmer, Phys. Rev. B **47**, 1397 (1993).

<sup>23</sup>C. Delerue, G. Allan, and M. Lannoo, Phys. Rev. B **48**, 11 024 (1993).

<sup>24</sup>J. P. Proot, C. Delerue, and G. Allan, Appl. Phys. Lett. **61**, 1948 (1993).